International Journal of Recent Development in Engineering and Technology
Website: www.ijrdet.com (ISSN 2347-6435 (Online) Volume 15, Issue 04, April 2026)

Comparative Study of Photocatalytic Degradation of Methylene Blue Dye with Copper Oxide Nanoparticles Synthesized From Various Plant Extracts

Shivani Gupta[1], Rimjhim Yadav[2], Himanshu Narayan[3], Rakesh K. Jain[1]

[1]*Shobhit Institute of Engineering & Technology, Modipuram, Meerut 250 110, India*
[2]*CSIR-National Physical Laboratory, Dr. K.S. Krishnan Marg, New Delhi 110 060, India*
[3]*Independent Researcher, Anant, 35 Purulia Road, Ranchi 834 001, India*

***Abstract*— Copper oxide nanoparticles (NPs) were synthesized starting with four different plant extracts, namely, that of Curry leaves, Moringa gum, Rudraksha leaves and Neem leaves, through a simple, green method precipitation. The photocatalytic properties of the samples were studied for the degradation of Methylene Blue (MB) dye, under sunlight as well as under UV irradiation. In this report, a comparative analysis of the degradation results in terms of the rate constants, and final percent concentration of the MB dye degraded, corresponding to each of the four samples under two types of irradiations has been presented. The best initial rate of degradation was observed with CuO NP samples synthesized with Moringa gum extract, which produced approximately 87% of the dye degradation in 180 min, under sunlight. Moreover, the CuO NPs synthesized using Neem leaves extract, produced close to 95% degradation of the MB dye in 180 min under sunlight, with a rate constant of 5.94×10^{-2} min^{-1}. The observed degradation may be attributed primarily to the process of photosensitization.**

***Keywords*— Photocatalysis, Nanoparticles, Green synthesis, Degradation.**

I. INTRODUCTION

The introduction of dyes into water has substantial adverse effects on human health. These dyes are frequently used in industries such as food, cosmetics, and textiles, with global production surpassing one million tons. [1]. The dyeing industry alone discharges approximately 7.5 metric tons of dye waste annually on a global scale. Textile dyes effect the aquatic habitat and may enter the food chain providing bioaccumulation and adversely affecting human health [2].

Traditional methods for treating water contaminated with dyes encompass physicochemical techniques such as coagulation, chemical precipitation, oxidation, irradiation, and absorption, as well as biological methods using bacteria, fungi, yeasts, and algae. Among these, adsorption stands out for its effectiveness and cost-efficiency [3].

Modern technologies for dye removal include advanced oxidation processes, adsorption, membrane techniques, and the use of photocatalytic reactors with nanomaterials. Nanoparticles, especially metal oxide semiconductors [4,5], have gained interest for their economic and eco-friendly synthesis methods and their effectiveness in breaking down a wide variety of pollutants in water [6,7].

Photocatalysis involves the use of light-triggered catalysis in a chemical reaction. Its efficiency relies on generating pairs of electrons and holes, and creating free radicals that drive the reaction. Photocatalytic oxidation involves two processes: photo-excitation and photo-sensitization.

Photo-excitation: As indicated by their nomenclature, in the process of photo-excitation, electrons experience elevation from the valence band to the conduction band when illuminated by light of a suitable wavelength. Following this, the resulting voids in the valence band interact with oxygen and hydroxide ions, resulting in the creation of highly reactive oxygen radicals that then interact with the contaminant.

Photo-sensitization: In the context of photo-sensitization, contaminants get adsorbed to the surface of the catalyst and subsequently absorb light radiation. This absorption prompts the activation of electrons, inducing the creation of a superoxide anion radical via the reduction of molecular oxygen. Simultaneously, the voids formed in the valence band interact with oxygen, water, and hydroxide ions, resulting in the production of highly active oxygen species that engage with the pollutants and degrade them.

Several metal-oxide nanoparticles act as photocatalysts, including ZnO, , TiO_2, CuO, and others due to their extraordinary chemical and physical properties [8,9]. Among these, CuO nanoparticles stand out for their impressive photocatalytic capabilities. They possess noteworthy magnetic, optical, electrical, and dye-absorption attributes.

International Journal of Recent Development in Engineering and Technology
Website: www.ijrdet.com (ISSN 2347-6435 (Online) Volume 15, Issue 04, April 2026)

Nevertheless, the chemical methods used to synthesize these nanoparticles have limitations such as lengthy reaction times, limited efficiency, and potential post-effects of toxicity [10]. As a result, the environmentally conscious synthesis of metal-oxide nanoparticles has gained considerable attention recently.

The use of plants to mediate the nanoparticles made of green synthesis proves to be cost-effective, safe, environmentally friendly, and employs straightforward techniques [10,11].

II. Materials And Methods

CuO NPs were synthesized through the method of chemical precipitation using extracts of Curry leaves, Moringa gum, Rudraksh leaves and Neem leaves. In the following section, we present a brief account of the preparation of plant extracts used in the synthesis, followed by the method employed.

A. Curry Leaves

Curry leaves, also named Murrayakoenigii belong to the family Rutaceae comprising of 150 genera and 1600 species [12,13]. It holds a significant role as a flavour enhancer not only in South India but across the entire country. The leaves possess a mild bitterness and subtle acidity, retaining their flavour even after undergoing the drying process. Originating from India, Bangladesh, Sri Lanka, and the Andaman Islands, its historical roots can be traced back to the 1st to 4th centuries AD, as documented in Tamil and Kannada literature. The distinctive aroma of curry leaves primarily emanates from compounds like pinene, sabinene, cadinol, caryophyllene, and cadiene. Various constituents of this plant have been harnessed for medicinal purposes, including the treatment of venomous bites, addressing calcium deficiency, and managing dysentery. The antioxidant properties of curry leaves have been explored using various solvents [14]. Extensive research has highlighted its remarkable attributes, encompassing antimicrobial, antiulcer, antioxidative, cytotoxic, phagocytic, and pharmacological activities [15].

The curry leaves were collected from the kitchen garden and about 100 g was washed and dipped in 150 ml of deionized water. It was boiled for an hour to get the complete leaf extract. The filtrate was centrifuged at 10,000 rpm, for 15 min and the supernatant was used as the extract.

B. Moringa gum

Moringa olifera Lam, also known as the horseradish tree, is a tropical tree with various regional names like drumstick tree, benzolive, kelor, mlongesaijhan, munga, and sajna. It has garnered attention in recent decades due to its exceptional medicinal and nutritional value [16]. Different parts of this tree serve as abundant sources of vitamins and minerals and have numerous pharmacological and biotechnological applications. Its seeds are widely employed in wastewater treatment due to their coagulation and sedimentation properties. Extensive research has been conducted on the chemical constituents of M. olifera stem, leaves, flowers, pods, and seeds, leading to the production of bioactive compounds, including phenolic acids, gallic acid, ellagic acid, and flavonoids, which exhibit antimicrobial properties [17,18,19]. Natural gum polysaccharides derived from this tree have gained significant utility in the biotechnology and pharmaceutical industries in recent years. While every part of the Moringa tree has its unique uses, this paper focuses on the extract of its gum, which possesses multiple properties, including antioxidants, astringency, and antipyretic effects, and is utilized in the treatment of syphilis, gastrointestinal problems, and rheumatism [20].

Fig. 1 Preparation of "CuO" NPs by Curry leaves extract

International Journal of Recent Development in Engineering and Technology
Website: www.ijrdet.com (ISSN 2347-6435 (Online) Volume 15, Issue 04, April 2026)

Moringa gum was collected from a local nursery and about 25 gm of the cleaned gum was boiled in 150 ml of deionized water for an hour.

The solution turns out to be sticky and quite thicker. The filtrate was centrifuged and the supernatant was collected as the extract.

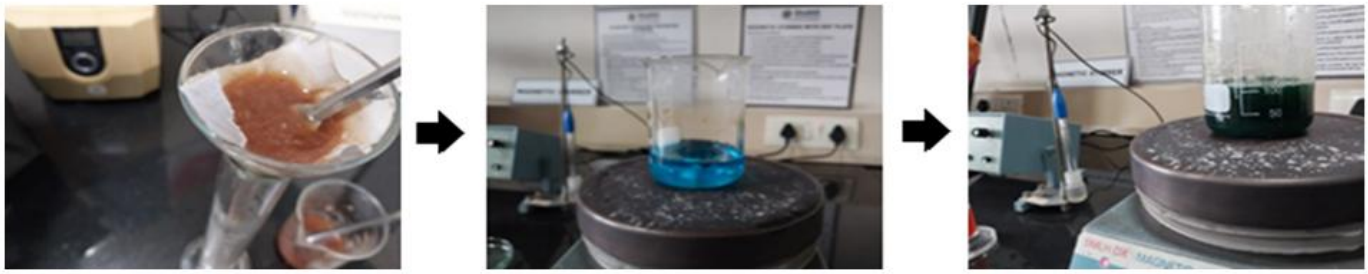

Fig. 2 Preparation of CuO NPs by Moringa gum extract

C. Rudraksha Leaves

Rudraksha, also recognized as the blueberry ash tree and scientifically named Elaeocarpus ganitrus, holds profound traditional and mythological significance. Throughout history, it has been employed for treating a variety of conditions, including stress, anxiety, nerve pain, epilepsy, and migraines [21]. Its leaves possess a slightly bitter taste, lack odour, and exhibit an oblong-lanceolate shape. Researchers have drawn attention to its anti-inflammatory and analgesic properties. The elemental composition of gases within Rudraksha includes 50% carbon, 31% oxygen, 18% hydrogen, and approximately 1% nitrogen.

When examined in various solvents, Rudraksha demonstrates antimicrobial, cytotoxic, and pharmacological activities [22]. This report focuses on the synthesis of copper nanoparticles using Rudraksha leaves for potential degradation applications.

Rudraksha leaves were taken from the campus of the Shobhit Institute of Engineering and Technology, Meerut freshly and washed with deionized water. 100 g of leaves were boiled in 150 ml of deionized water for an hour, centrifuged and filtered.

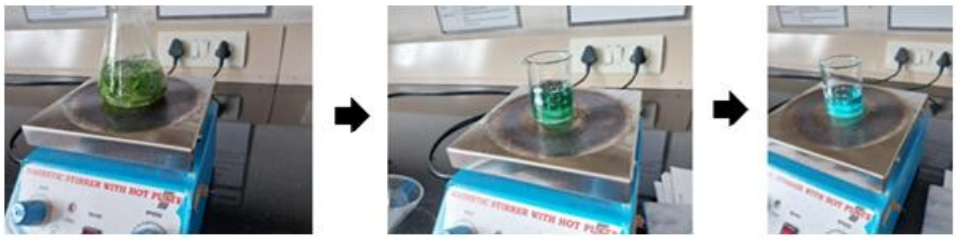

Fig. 3 Preparation of "CuO" NPs by Rudraksh leaves extract

D. Neem Leaves

Neem, also named Azadirachta indica, margosa, and Indian lilac is a member of the Meliaceae family [23]. Neem tree is considered to be a divine tree in India owing to its extraordinary medicinal properties [24,25]. It has gained importance worldwide because of its medicinal, anti-inflammatory, antiulcer, antimalarial and immunomodulatory properties.

It originally belonged to the Indian subcontinent and a few parts of Southern Asia. Neem word is derived from the Sanskrit word nimba. Almost 140 compounds are extracted from various parts of the neem tree. It is believed to be originated in Assam and Burma [26]. All its parts such as stems, roots, fruits, bark flowers, seeds etc. are used traditionally for the treatment of infections. It is used commonly in Ayurvedic, Unani and Homeopathic medicines [27].

International Journal of Recent Development in Engineering and Technology
Website: www.ijrdet.com (ISSN 2347-6435 (Online) Volume 15, Issue 04, April 2026)

Fig. 4 Preparation of "CuO" NPs by Neem leaves extract.

Neem leaves were collected from a tree in my garden, and washed with deionized water. 100gm of the leaves were boiled in 150 ml of water for an hour. The extract was filtered and centrifuged for 15 min to obtain the supernatant.

III. Green Synthesis Of Copper-Oxide NPs

All chemical reagents used in the synthesis of NPs were of analytical grade, and utilized without further modification, and ultra-pure water was employed throughout the procedures. Sodium hydroxide (NaOH) was sourced from the college laboratory, while copper sulfate ($CuSO_4$) was acquired from Fischer Chemicals.

Different concentrations of copper sulphate pentahydrate ($CuSO_4 5H_2O$) were prepared such as 0.5 M, 1M and 1.5 M solutions. The plant extract was added to the solution dropwise slowly by continuously stirring and heated at a temperature of 50-60 ℃. It was left for 24 hours undisturbed at room temperature. It was filtered and the final residue was calcinated at 150 ℃. The precipitate was washed a few times and dried in the oven at 150 ℃ for an hour till the powder was completely dry into fine powder.

A. Characterization and measurements

X-ray diffraction (XRD) was performed on a Rigaku Miniflex 600 Diffractometer equipped with Cu-Kα radiation for structural analysis. Scanning Electron Microscopy (SEM) was done at National Physical Laboratory, New Delhi, India using a Tescan Magna GMH unit. The UV-visible spectroscopy was carried out on a PC-based double beam Spectrophotometer 2206 from Systronics India.

B. Photocatalytic activity under sunlight and UV light

The photocatalytic performance of green-synthesized CuO nanoparticles (NPs) was investigated for the degradation of Methylene Blue (MB) dye in an aqueous solution under sunlight and UV light separately.

The absorption peak obtained from the UV-Vis spectra of the experimental solution has a direct correlation with the dye concentration. Investigations were performed for the various molar concentrations of the solution. However, in this paper, we present the comparative results for molar concentrations 1 for all the four CuO NP samples. The steps followed are described below.

A solution of 50 mL was prepared for each sample, with a concentration of 0.05 g per 50 mL. The solution was taken in a beaker for the photocatalysis experiment and placed in the bright sunlight of summer in Meerut (around 30-34 °C) for sunlight exposure. On the other hand, similar solution in another beaker was kept in a UV chamber under 250 nm wavelength exposure. About 5 mL of the solution was taken out every half an hour, from both sunlight and UV light irradiated experimental set up, and the UV-Vis spectroscopy was carried out. The gradually decreasing intensities of the absorption peaks showed the lowering concentration of the dye molecules with time. The observations were taken for a continuous 180 min duration of experiment under regular stirring.

C. Data analysis

Normalized relative concentration of MB dye in the solution estimated from the height of peaks in the UV-Vis curves, was plotted as a function of time and degradation curves were obtained. As expected, the degradation curves are characterized by first-order reaction kinematics, mathematically represented by the equation,

$$\ln\left(\frac{C}{C_0}\right) = -k_{\text{obs}}t$$

where C_0 is the starting concentration and C is the instantaneous concentration of the dye in the solution after time t, and k_{obs} is the first order rate constant, or the rate of degradation. The negative sign implies degradation.

International Journal of Recent Development in Engineering and Technology
Website: www.ijrdet.com (ISSN 2347-6435 (Online) Volume 15, Issue 04, April 2026)

Obviously, if natural log of normalized concentration of dye, $\ln(C/C_0)$, is plotted against time, it will produce a straight line with its slope immediately giving the value of rate constant k_{obs}.

In the next section, we present the UV-Vis curves recorded at different time intervals showing gradually decreasing concentration of MB dye.

Also shown are the degradation plots $\ln(C/C_0)$ against time t, together with a graph in the inset showing percentage degradation of the dye $(C/C_0) \times 100$ plotted against time t.

IV. Results And Discussion

The X-ray diffraction profiles of the CuO NP samples synthesized using various plant extracts are depicted in Figure 5. The most prominent peaks of CuO are easily distinguishable, appearing around 2θ angles of approximately 36.0° and 39.1° in all the four samples synthesized from different plant extracts. These peaks correspond to the double reflections of {(002) and (-111)} and {(111) and (200)} of the monoclinic CuO unit cell of the Cc space group.

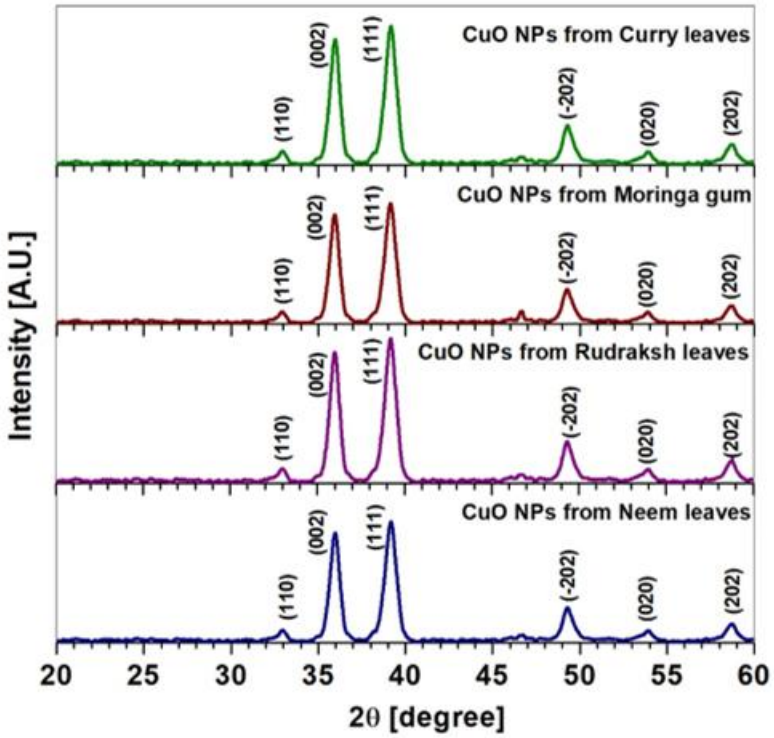

Fig. 5 Figure XRD profiles of CuO NPs synthesized from various plant extracts.

Obvious broadening of the most prominent peaks, indicates the formation of nanoparticles. Apparently, the plant extracts used in the process of synthesis perform the dual function, serving as a reducing, as well as the capping-agent during the synthesis of nanoparticles.

By employing Gaussian fitting on the most prominent XRD peaks and applying the Debye-Scherrer formula, $D = k\lambda/(\beta\cos\theta)$, the average crystallite size of the samples was estimated. The mean crystallite size of the samples prepared by extracts of Curry leaves, Moringa gum, Rudraksha leaves and Neem leaves were estimated to be nearly 13.7 nm, 13.2 nm, 13.5 nm and 14.0 nm, respectively.

Therefore, a rounded-off average of 14 nm was taken to be the crystallite size for all the samples.

Figure 6 shows representative SEM images of all the four CuO NP samples prepared from various plant extracts. The surface morphology of all the samples appears to be rough. It is also obvious that the crystallites have clustered into bigger particles of roughly a few tens of nm in size, which have further agglomerated into larger grains of approximately 100 nm size. The rough surface morphology is expected to assist degradation through photosensitization due to the availability of larger specific surface area for adsorption of dye molecules.

International Journal of Recent Development in Engineering and Technology
Website: www.ijrdet.com (ISSN 2347-6435 (Online) Volume 15, Issue 04, April 2026)

Figure 6 shows representative SEM images of all the four CuO NP samples prepared from various plant extracts. The surface morphology of all the samples appears to be rough. It is also obvious that the crystallites have clustered into bigger particles of roughly a few tens of nm in size, which have further agglomerated into larger grains of approximately 100 nm size. The rough surface morphology is expected to assist degradation through photosensitization due to the availability of larger specific surface area for adsorption of dye molecules.

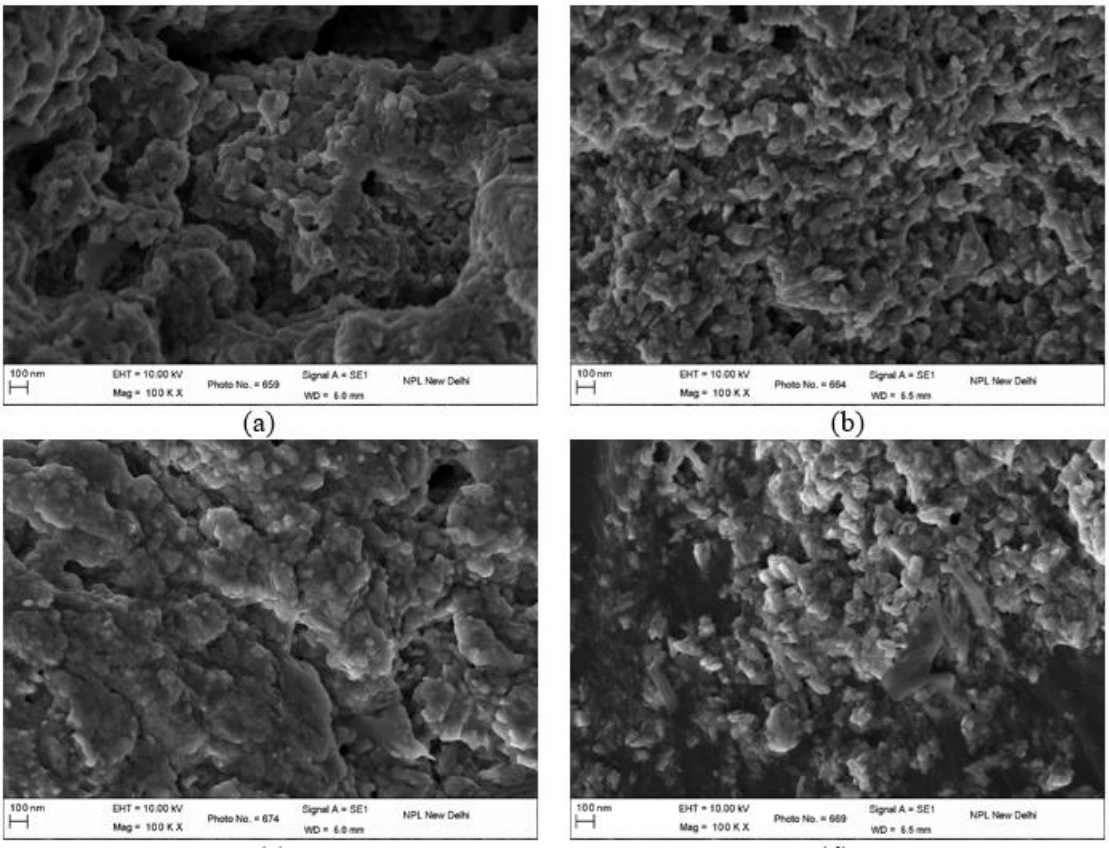

Fig. 6. SEM images of CuO NPs synthesized from various plant extracts: (a) Curry leaves, (b) Moringa gum, (c) Rudraksh leaves, and (d) Neem leaves.

Figure 6 shows representative SEM images of all the four CuO NP samples prepared from various plant extracts. The surface morphology of all the samples appears to be rough. It is also obvious that the crystallites have clustered into bigger particles of roughly a few tens of nm in size, which have further agglomerated into larger grains of approximately 100 nm size. The rough surface morphology is expected to assist degradation through photosensitization due to the availability of larger specific surface area for adsorption of dye molecules.

Figure 6 shows representative SEM images of all the four CuO NP samples prepared from various plant extracts. The surface morphology of all the samples appears to be rough.

It is also obvious that the crystallites have clustered into bigger particles of roughly a few tens of nm in size, which have further agglomerated into larger grains of approximately 100 nm size. The rough surface morphology is expected to assist degradation through photosensitization due to the availability of larger specific surface area for adsorption of dye molecules.

International Journal of Recent Development in Engineering and Technology
Website: www.ijrdet.com (ISSN 2347-6435 (Online) Volume 15, Issue 04, April 2026)

Figure 6 shows representative SEM images of all the four CuO NP samples prepared from various plant extracts. The surface morphology of all the samples appears to be rough. It is also obvious that the crystallites have clustered into bigger particles of roughly a few tens of nm in size, which have further agglomerated into larger grains of approximately 100 nm size.

The rough surface morphology is expected to assist degradation through photosensitization due to the availability of larger specific surface area for adsorption of dye molecules.

A. Degradation results under Sunlight

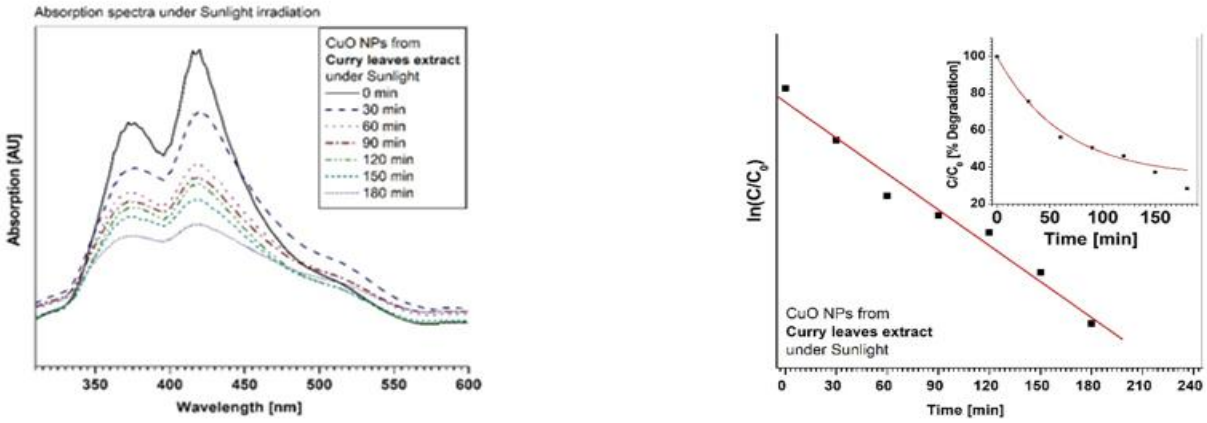

(a) (b)

Fig. 7. Degradation of MB dye with CuO NPs synthesized from Curry leaves extract under sunlight. (a) UV-Vis absorption spectra at different time intervals, and (b) Normalized concentration of MB, with original percent degradation data (inset), observed at different time intervals.

Figure 7 (a) shows the UV-Vis absorption spectra for MB dye with CuO NPs from Curry leaves extract under sunlight. The degradation curve showing reduction of the concentration of MB with time is shown in the inset of figure 7 (b) together with the plot of normalized concentration as a function of time. Final degradation percentage observed after 180 min was nearly 73% with a first order rate constant of approximately 6.45×10^{-3} min^{-1}. It was also noted that 50% of the MB dye was degraded in about 70 min.

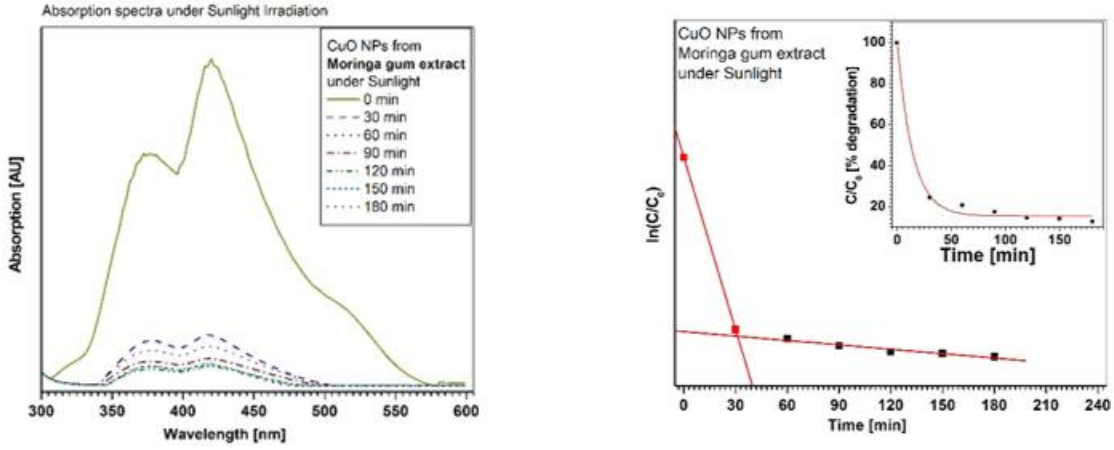

(a) (b)

Fig. 8. Degradation of MB dye with CuO NPs synthesized from Moringa gum extract under sunlight. (a) UV-Vis absorption spectra at different time intervals, and (b) Normalized concentration of MB, with original percent degradation data (inset), observed at different time intervals

International Journal of Recent Development in Engineering and Technology
Website: www.ijrdet.com (ISSN 2347-6435 (Online) Volume 15, Issue 04, April 2026)

The figure 8 (a) shows the UV-Vis absorption spectra for MB dye with CuO NPs from Moringa gum extract under sunlight and the figure 8 (b) shows the normalized concentration of MB dye as a function of time, along with the original degradation curve (inset). A very good final degradation percentage of nearly 87% was observed in 180 min. However, the process of degradation appears to have taken place in two distinct regimes. To make it obvious, we fitted the first couple of points, occurring within first 40 min, when the dye concentration has already reduced by more than 70% of the starting value, and estimated the initial rate constant, which came out to be 4.67×10^{-2} min^{-1}.

The remaining points, corresponding to the final 140 min, were fitted separately to estimate the final rate constant of nearly 3.94×10^{-3} min^{-1}. The difference of an of order of magnitude between the values of two rate constants is interesting.

The UV-Vis absorption spectra for MB dye with CuO NPs from Rudraksh leaves extract under sunlight is shown in figure 9 (a). A final degradation percentage of nearly 70% in 180 min with a slow first order, rather uniform, rate constant of 6.4×10^{-3} min^{-1}, was estimated. Due to such slow rate of degradation, the sample could degrade the dye to half of its initial concentration in sufficiently longer time of around 100 min.

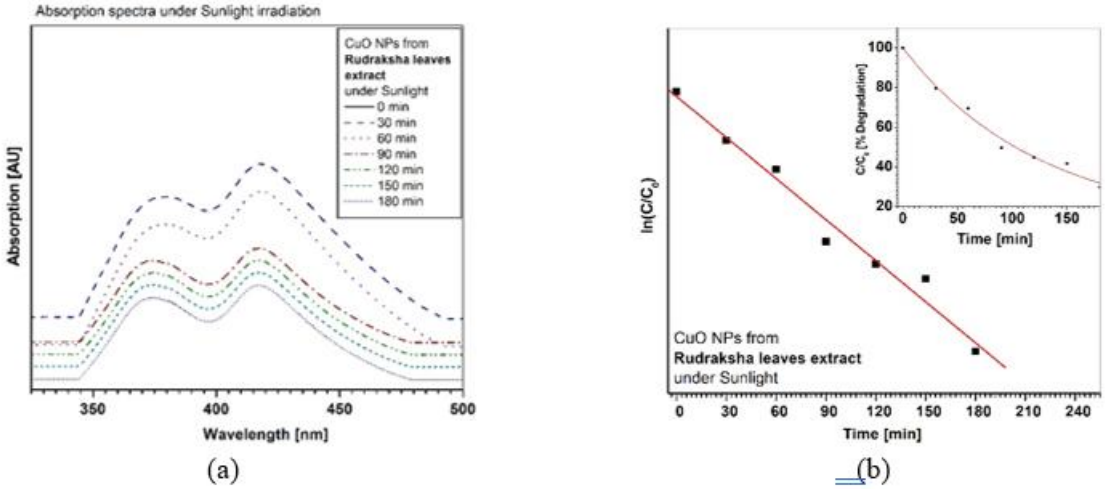

Fig. 9. Degradation of MB dye with CuO NPs synthesized from Rudraksha leaves extract under sunlight. (a) UV-Vis absorption spectra at different time intervals, and (b) Normalized concentration of MB, with original percent degradation data (inset), observed at different time intervals.

The UV-Vis absorption spectra for MB dye with CuO NPs from Neem leaves extract for degradation under sunlight is depicted in figure 10 (a). The final degradation percentage after 180 min, as noticed from the inset of figure 10 (b) was a good 95%.

A very fast first order initial rate constant calculated separately for first 60 min, and the final rate constant for the next 120 min, were 5.94×10^{-2} min^{-1} and 7.72×10^{-3} min^{-1}, respectively. These values are the best among all four types of CuO NPs investigated in this work.

International Journal of Recent Development in Engineering and Technology
Website: www.ijrdet.com (ISSN 2347-6435 (Online) Volume 15, Issue 04, April 2026)

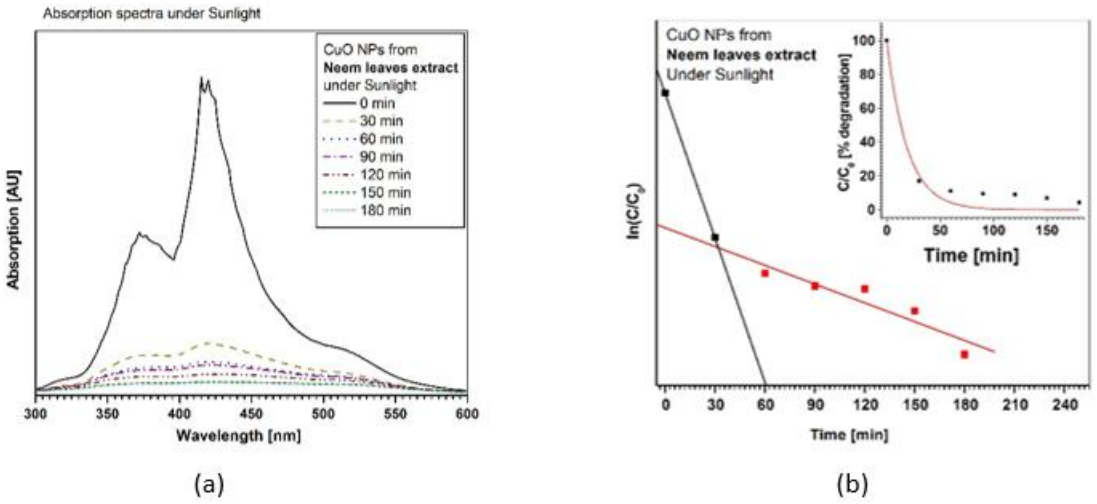

Fig. 10. Degradation of MB dye with CuO NPs synthesized from Neem leaves extract under sunlight. (a) UV-Vis absorption spectra at different time intervals, and (b) Normalized concentration of MB, with original percent degradation data (inset), observed at different time intervals.

B. Degradation results under UV irradiation

Figure 11 (a) shows the UV-Vis absorption spectra for MB dye with CuO NPs from Curry leaves extract under UV light. As evident from the original degradation data plotted in the inset of figure 11 (b), the final degradation percentage was around 65% in 180 min, and the rate of degradation was estimated to be around 4.87×10^{-3} min^{-1}. This sample took a nearly 80 min to degrade the dye to half of its initial concentration.

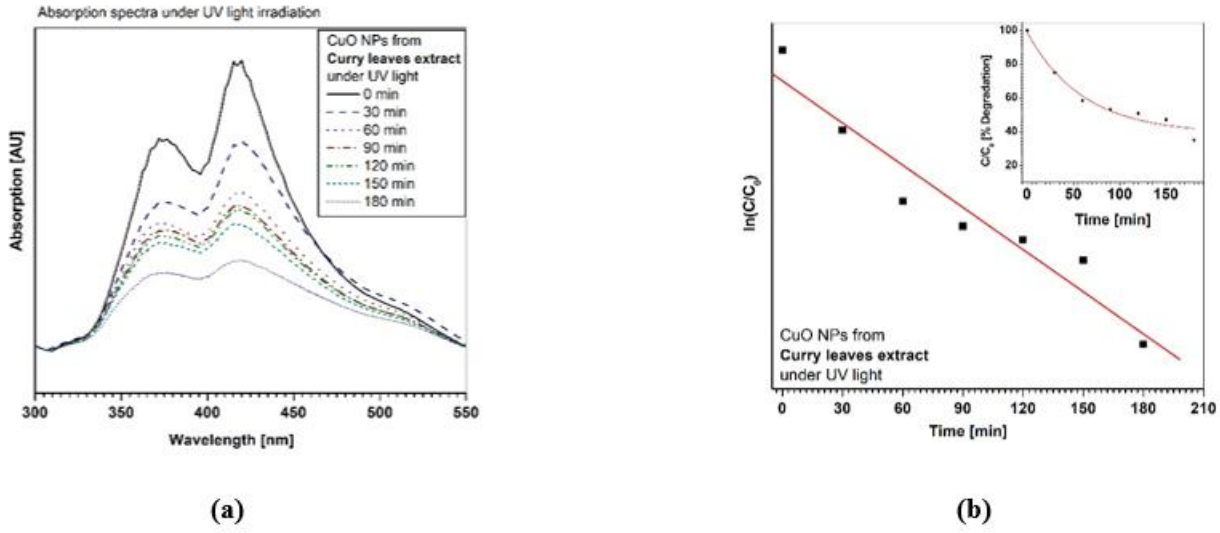

Fig. 11. Degradation of MB dye with CuO NPs synthesized from Curry leaves extract under UV irradiation. (a) UV-Vis absorption spectra at different time intervals, and (b) Normalized concentration of MB, with original percent degradation data (inset), observed at different time intervals.

International Journal of Recent Development in Engineering and Technology
Website: www.ijrdet.com (ISSN 2347-6435 (Online) Volume 15, Issue 04, April 2026)

Moringa gum based CuO NPs showed better degradation under UV irradiation also. The results are presented in figure 12 as UV-Vis absorption spectra (a) and degradation with respect to time. After 180 min, as much as 80% of the dye was finally degraded, with a faster rate of 4.68×10^{-2} min^{-1} initially (calculated separately for first 50 min) but eventually slowing down to around 1.11×10^{-3} min^{-1} in the next 140 min.

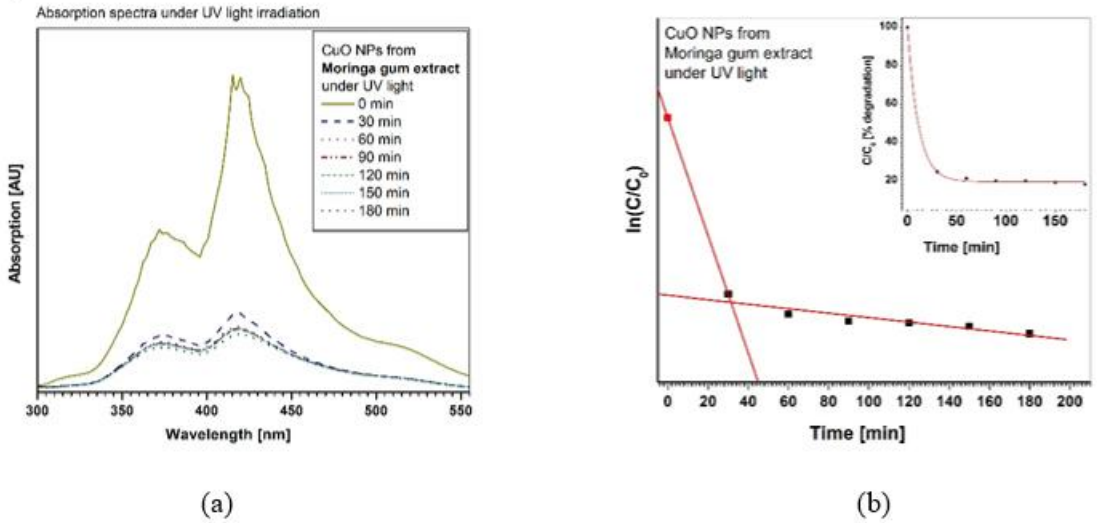

Fig. 12. Degradation of MB dye with CuO NPs synthesized from Moringa gum extract under UV irradiation. (a) UV-Vis absorption spectra at different time intervals, and (b) Normalized concentration of MB, with original percent degradation data (inset), observed at different time intervals.

CuO NPs from Rudraksha leaves extract could not degrade the dye beyond half of its starting concentration under UV irradiation. Results are shown in figure 12. For these samples, with a very slow rate of 5.86×10^{-3} min^{-1}, the degradation curve flattens after 90 min to around 45%, which eventually becomes the final degradation observed.

Just to get an idea about the flattening, the last four points were fitted with a straight line and the rate constant was estimated to be around 7.30×10^{-4} min^{-1}, which is two orders of magnitude slower than the initial rate. As a result, the dye could not be degraded even to half of the starting concentration.

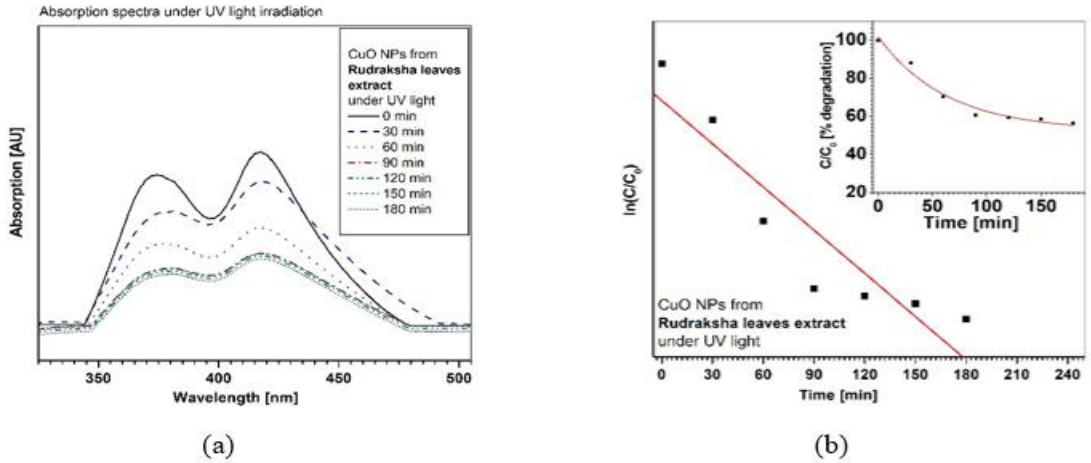

Fig. 13. Degradation of MB dye with CuO NPs synthesized from Rudraksh leaves extract under UV irradiation. (a) UV-Vis absorption spectra at different time intervals, and (b) Normalized concentration of MB, with original percent degradation data (inset), observed at different time intervals.

International Journal of Recent Development in Engineering and Technology
Website: www.ijrdet.com (ISSN 2347-6435 (Online) Volume 15, Issue 04, April 2026)

Figure 14 shows the UV-Vis absorption spectra for MB dye with CuO NPs from Neem leaves extract under UV irradiation. Starting with a very fast rate of around were 5.82×10^{-2} min^{-1} up to around the first 60 min, the samples finally degraded close to 90% of the dye in 180 min and even the final rate was approximately 9.85×10^{-3} min^{-1}.

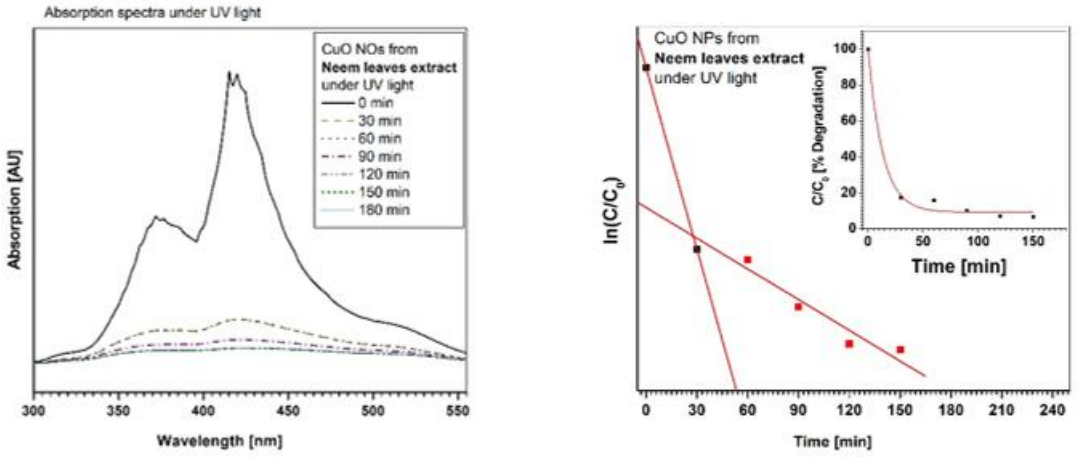

(a) (b)

Fig. 14. Degradation of MB dye with CuO NPs synthesized from Neem leaves extract under UV irradiation. (a) UV-Vis absorption spectra at different time intervals, and (b) Normalized concentration of MB, with original percent degradation data (inset), observed at different time intervals.

A summary of the degradation results is given in Table 1. Out of the two irradiation types, the sunlight seems to be the one leading to better degradation of MB dye. This can be attributed to the wide range of excitation wavelength available in the solar spectrum, as the wavelengths nicely matching with the direct and indirect bandgaps of the catalyst are highly probable. Through the process of photoexcitation, it favours the generation of e^-/h^+ pairs, which supports the degradation.

Further aided by the nano-sized particles with rough surface morphology, which backs photosensitization due to larger specific surface area, the whole process leads to a very effective degradation of the dye. In contrast, under the UV irradiation, a very limited portion of wavelengths is made available for photoexcitation, which may be the reason for the poorer performance of the photocatalysts.

International Journal of Recent Development in Engineering and Technology
Website: www.ijrdet.com (ISSN 2347-6435 (Online) Volume 15, Issue 04, April 2026)

Table I
Degradation of MB dye with CuO NPs using different plant extracts

Table I : Degradation of MB dye with CuO NPs using different plant extracts					
Plant Extract used	Irradiation type	Degradation %	$t_{1/2}$ min	Initial rate constant min^{-1}	Final rate constant min^{-1}
Curry leaf	UV light	65	80	4.87×10^{-3}	4.87×10^{-3}
	Sunlight	73	70	6.45×10^{-3}	6.45×10^{-3}
Moringa gum	UV light	80	10	4.68×10^{-2}	1.11×10^{-3}
	Sunlight	87	12	4.67×10^{-2}	3.94×10^{-3}
Rudraksh leaf	UV light	45	180	5.86×10^{-3}	7.30×10^{-4}
	Sunlight	70	100	6.40×10^{-3}	6.40×10^{-3}
Neem leaf extract	UV light	93	17	5.82×10^{-2}	9.85×10^{-3}
	Sunlight	95	20	5.94×10^{-2}	7.72×10^{-3}

Among the four types of CuO NPs prepared using four different plant extracts, the best final degradation of 95% in 180 min under sunlight was produced by the one with Neem leaves extract. Expectedly, the rate associated with this was also the best among all samples. In terms of the initial degradation, the CuO NPs synthesized from Moringa gum seem to be the fastest as it degraded the dye to nearly 50% of the starting concentration in just about 12 min under sunlight, even though the value of rate constant was only the second best. A careful analysis of the rates together with the particle size of these two top-performing samples infers a very interesting deduction. As mentioned earlier, the average crystallite size estimated for the Moringa gum and Neem leaves based samples were nearly 13 nm and 14 nm, respectively. This small difference in crystallite size warrants slightly better photosensitization in the CuO NPs synthesized from Moringa gum and therefore, an improved degradation. This conclusion is supported by the results of degradation obtained with these NPs under UV irradiation support also.

Finally, the results also indicate another important intuitive inference that since the rough surface morphology together with smaller particle size implies larger specific surface area, and thus supports better photosensitization, the initial rate of photocatalytic degradation may be higher in some photocatalysts.

This is so because photosensitization is the dominating route of photocatalytic degradation at the beginning. Once the pollutant molecules adsorbed on the catalyst particles get degraded, the photoexcitation route takes over.

V. Conclusions

CuO NPs were synthesized from four different plant extracts and their photocatalytic activities were investigated for the degradation of MB dye under sunlight and UV irradiation. The CuO NPs synthesized from Neem leaves extract produced the best overall degradation (close to 95% in 180 minutes), The samples obtained from Moringa gum extract degraded the pollutant very fast at the beginning reducing nearly 50% of the initial concentration of MB in just 12 minutes. Although these NPs had a slightly slower overall degradation rate, their smaller average crystallite size of approximately 13 nm as compared to that of 14 nm for Neem based NPs, likely contributed to a faster initial degradation. The study suggests that a rough surface morphology and smaller particle size might lead to a higher initial degradation rate by providing more specific surface area for pollutants to get adsorbed and subsequently get degraded. This highlights the importance of considering both particle size and surface properties when designing photocatalysts. Further modifications are still possible through appropriate doping of the photo-catalyst. The work along these lines is currently on.

ACKNOWLEDGEMENTS

The authors would like to acknowledge the Dr. S.P. Singh and Mr. Vinod Tanwar at CSIR-NPL, New Delhi, India for their unconditional help and support with electron microscopy.

REFERENCES

[1] Maheshwari K., Agrawal M. and Gupta A. B. 2021. Dye Pollution in Water and Wastewater. In: Muthu, S.S., Khadir, A. (eds) Novel Materials for Dye-containing Wastewater Treatment. Sustainable Textiles: Production, Processing, Manufacturing & Chemistry.

[2] Al-Tohamy R., Ali S. S., Li F., Okasha K. M., Mahmoud Y. A.-G., Elsamahy T., Jiao H. and Fu Y. Sun J. 2022. A critical review on the treatment of dye-containing wastewater: Ecotoxicological and health concerns of textile dyes and possible remediation approaches for environmental safety

[3] Sardar M., Manna M., Maharana M. and Sen S. 2021. Remediation of Dyes from Industrial Wastewater Using Low-Cost Adsorbents.

[4] Li Y., Cui W., Liu L., Zong R., Yao W., Liang Y. and Zhu Y. 2016. Removal of Cr (VI) by 3D TiO2-graphene hydrogel via adsorption enriched with photocatalytic reduction.

[5] Kudo A. and Miseki Y. 2009. Heterogeneous photocatalyst materials for water splitting.

[6] Naseri A., Samadi M., Mahmoodi N. M., Pourjavadi A., Mehdipour H. and Moshfegh A. Z. 2017. Tuning composition of electrospun ZnO/CuO nanofibers: toward controllable and efficient solar photocatalytic degradation of organic pollutants.

[7] Hoffmann M. R., Martin S. T., Choi W. and Bahnemann D. W. 1995. Environmental applications of semiconductor photocatalysis.

[8] Kabra K., Chaudhary R. and Sawhney R. L. 2004. Treatment of hazardous organic and inorganic compounds through aqueous-phase photocatalysis: a review.

[9] Raizada P., Sudhaik A., Patial S., Hasija V., Khan A. A. P., Singh P., Gautam S., Kaur M. and Nguyen V.-H. 2020. Engineering nanostructures of CuO-based photocatalysts for water treatment: Current progress and future challenges.

[10] Eswaan S. G., Narayan H. and Vasimalai N. 2021. Reductive photocatalytic degradation of toxic aniline blue dye using green synthesized banyan aerial root extract derived silver nanoparticles.

[11] Gupta S., Narayan H. and Jain R. K. 2023. A review of some metal-oxide based nanocomposites for photocatalytic treatment of wastewater.

[12] Sangam S., Naveed A., Athar M., Prathyusha P., Moulika S. and Lakshmi S. 2015. A Study on Functional Measures in Patients with Stroke.

[13] Bhusal D. and Thakur D. P. 2021. Curry Leaf: A Review, Reviews in Food and Agriculture.

[14] Zahrah A. 2022. Green synthesis of copper oxide nanoparticles CuO NPs from Eucalyptus Globoulus leaf extract: Adsorption and design of experiments.

[15] Singh S., More P. K. and Mohan S. M. 2014. CURRY LEAVES (Murraya koenigii Linn. Sprengal)- A MIRCALE PLANT.

[16] Arulselvan P. and Subramanian S. P. 2007. "Beneficial effects of Murraya koenigii leaves on antioxidant defense system and ultrastructural changes of pancreatic beta-cells in experimental diabetes in rats".

[17] Fahey J. 2005. A Taylor & Francis Group LLC.

[18] Brilhante R. S. N., Sales J., Pereira V. S., Castelo-Branco D. C.M., Cordeiro R. A., Sampaio C. M., Paiva M .N., Feitosa dos Santos J. B., Sidrim J.J.C. and Rocha M.F. G. 2017. Research advances on the multiple uses of Moringa oleifera: A sustainable alternative for socially neglected population.

[19] Bhattacharya A., Tiwari P., Sahu P. K. and Kumar S. 2018. A review of the phytochemical and pharmacological characteristics of Moringa oleifera.

[20] Mbikay M. 2012. Therapeutic Potential of Moringa oleifera Leaves in Chronic Hyperglycemia and Dyslipidemia: A Review.

[21] Kumari L., Baghel M., Panda S., Sakure K., Giri T. K. and Badwaik H. 2021. Reference Series in Phytochemistry.

[22] Hardainiyan S., Nandy B. C., Kumar K. 2015. Elaeocarpus Ganitrus (Rudraksha): A Reservoir Plant with their Pharmacological Effects.

[23] Amritalingam M. 2001. Neem Tree- A Review.

[24] Reddy I. V. S. and Palagani N. 2022. Neem (Azadirachta indica): A Review on Medicinal Kalpavriksha.

[25] Alzohairy M. A. 2016. Therapeutics Role of Azadirachta indica (Neem) and Their Active Constituents in Diseases Prevention and Treatment.

[26] Subapriya R. and Nagini S. 2005. Medicinal properties of neem leaves: a review.

[27] National Research Council .1992. *Neem: A Tree for Solving Global Problems*. Washington, DC: The National Academies Press.

List of figures and table

Fig.1 Preparation of CuO NPs by Curry leaves extract

Fig.2 Preparation of CuO NPs by Moringa gum extract.

Fig.3 Preparation of CuO NPs by Rudraksh leaves extract

Fig.4 Preparation of CuO NPs by Neem leaves extract.

Fig.5 Figure XRD profiles of CuO NPs synthesized from various plant extracts.

Fig.6 SEM images of CuO NPs synthesized from various plant extracts: (a) Curry leaves, (b) Moringa gum, (c) Rudraksh leaves, and (d) Neem leaves.

Fig.7 Degradation of MB dye with CuO NPs synthesized from Curry leaves extract under sunlight. (a) UV-Vis absorption spectra at different time intervals, and (b) Normalized concentration of MB, with original percent degradation data (inset), observed at different time intervals.

Fig.8 Degradation of MB dye with CuO NPs synthesized from Moringa gum extract under sunlight. (a) UV-Vis absorption spectra at different time intervals, and (b) Normalized concentration of MB, with original percent degradation data (inset), observed at different time intervals.

Fig.9 Degradation of MB dye with CuO NPs synthesized from Rudraksha leaves extract under sunlight. (a) UV-Vis absorption spectra at different time intervals, and (b) Normalized concentration of MB, with original percent degradation data (inset), observed at different time intervals.

Fig.10 Degradation of MB dye with CuO NPs synthesized from Neem leaves extract under sunlight. (a) UV-Vis absorption spectra at different time intervals, and (b) Normalized concentration of MB, with original percent degradation data (inset), observed at different time intervals.

Fig.11 Degradation of MB dye with CuO NPs synthesized from Curry leaves extract under UV irradiation. (a) UV-Vis absorption spectra at different time intervals, and (b) Normalized concentration of MB, with original percent degradation data (inset), observed at different time intervals.

Fig.12 Degradation of MB dye with CuO NPs synthesized from Moringa gum extract under UV irradiation. (a) UV-Vis absorption spectra at different time intervals, and (b) Normalized concentration of MB, with original percent degradation data (inset), observed at different time intervals.

Fig.13 Degradation of MB dye with CuO NPs synthesized from Rudraksh leaves extract under UV irradiation. (a) UV-Vis absorption spectra at different time intervals, and (b) Normalized concentration of MB, with original percent degradation data (inset), observed at different time intervals.

Fig.14 Degradation of MB dye with CuO NPs synthesized from Neem leaves extract under UV irradiation. (a) UV-Vis absorption spectra at different time intervals, and (b) Normalized concentration of MB, with

original percent degradation data (inset), observed at different time intervals.

Table I Degradation of MB dye with CuO NPs using different plant extracts